



# Establishment of Three-Dimensional Mesoscale Model of Concrete and Simulation of Uniaxial Mechanical Behavior

Lin Hua<sup>1\*</sup>, Jiwu Yang<sup>2</sup>, Yali Wang<sup>2</sup>, Yanbao Huang<sup>2</sup>, Liu T B<sup>2</sup>

<sup>1</sup>School of Civil Engineering, Lanzhou Jiaotong University, Lanzhou 730070, China

<sup>2</sup>China Railway First Group Co., Ltd, Xianyang 712000, China

\* E-Mail: 2625450709@qq.com

**Abstract.** This study investigates the mesoscale damage and mechanical behavior of concrete under loading by establishing a three-dimensional mesoscale model and conducting uniaxial compression simulations. Traditional methods are insufficient in accurately capturing crack propagation, stiffness degradation, and stress distribution within concrete. However, mesoscale numerical simulation methods, known for their efficiency and precision, have emerged as effective tools for studying the failure process of concrete. Based on the random distribution characteristics of aggregate size and spatial position, this research employs Python for secondary development of ABAQUS, integrating micromechanics of composite materials to develop algorithms for generating and placing coarse aggregates. The Mersenne Twister algorithm is utilized to generate random numbers, ensuring the randomness of aggregate placement. Additionally, the study adopts a three-dimensional aggregate grading theory based on the Fuller curve to optimize the distribution of aggregates. During model construction, polyhedral aggregates are generated using point-based random shape control methods and planar topology techniques, and the convexity of aggregates is determined using vector methods to avoid the formation of sharp angles and thin flake-like aggregates. Interference between aggregates and between aggregates and boundaries is judged by calculating the distances between aggregate centers and between aggregates and boundaries, enabling the batch placement of aggregates. Simulation results indicate that concrete with different aggregate shapes exhibits distinct stress-strain relationships and failure modes. Concrete with spherical aggregates has the highest peak strength and can still withstand certain stress after failure, while concrete with irregular polyhedral aggregates shows more rapid crack development and lower residual strength. The findings of this study provide a theoretical basis and reference for the engineering design and performance evaluation of concrete structures.

**Keywords:** Microscopic models of concrete; aggregate modeling; uniaxial compression

## 1 Introduction

When concrete is subjected to forces, the internal stress and damage are complex. Traditional analytical solutions and experimental methods have difficulty accurately capturing crack propagation, stiffness degradation, and stress distribution[1,2,9]. Moreover, experiments are prone to deviations, time-consuming, and resource-intensive. However, with the development of computer technology and micromechanical finite element theory, mesoscale numerical simulation methods have emerged as effective means to study the failure process. These methods can intuitively reflect mesoscale damage and crack propagation, track damage inversion across scales, and comprehensively grasp the structural failure process from the micro to the macro level. Based on reasonable models and precise data, they can partially replace experiments, avoiding experimental limitations and human interference, and efficiently simulate the mechanical behavior of structures under different working conditions, providing efficient ideas for engineering design and evaluation.

In this study, based on the random distribution characteristics of aggregate size and spatial position, Python was used for secondary development of ABAQUS, combined with micromechanics of composite materials. Algorithms for the generation and placement of coarse aggregates were developed. The constraints of non-overlapping aggregates and separation between aggregates and concrete boundaries were followed, and random functions were used to ensure the randomness of the placement process.

## 2 Random Algorithm Model and Grading Theory

### 2.1 Mersenne Twister Algorithm

The coarse aggregate phase in concrete is uncertain in position and is randomly distributed. Therefore, the first step in creating a mesoscale numerical model is to generate random aggregates, which requires the use of random numbers. In this study, Python was used for secondary development, and the random module was utilized to generate random numbers. The random module primarily uses the Mersenne Twister algorithm to generate pseudo-random numbers. The Mersenne Twister is a very famous pseudo-random number generation algorithm proposed by Makoto Matsumoto and Takuji Nishimura in 1997. It is widely used due to its excellent statistical properties and long period.

The name of the Mersenne Twister algorithm comes from the length of its period, which is a Mersenne prime. Mersenne primes are primes of the form  $2^p-1$ , where  $p$  is also a prime number. The period length of the algorithm is  $2^{19937}-1$ , which is a very large number, ensuring that the generated sequence of random numbers will not repeat for a very long time. The generated random numbers also have good statistical uniformity and independence, making them suitable for applications such as simulation and random sampling. The algorithm is highly efficient in implementation, capable of generating a large number of random numbers in a short period of time. This is also the

core of efficient random number generation in this study's computational implementation.

### 2.2 Three-Dimensional Aggregate Grading Based on the Fuller Curve

Aggregate grading refers to the size and distribution proportion of aggregate particles in concrete. An optimal aggregate grading should meet specific criteria and significantly influences the performance of concrete during its mix design. Aggregate grading that conforms to a continuous grading curve helps improve the density and strength of concrete. Currently, for numerical modeling at the mesoscale of concrete, one of the most ideal grading theories is the grading curve proposed by American scholar Fuller W.B. and his colleagues, based on extensive experiments(As shown in Figure 1), which aims to achieve the minimum porosity and maximum density of the mixture.

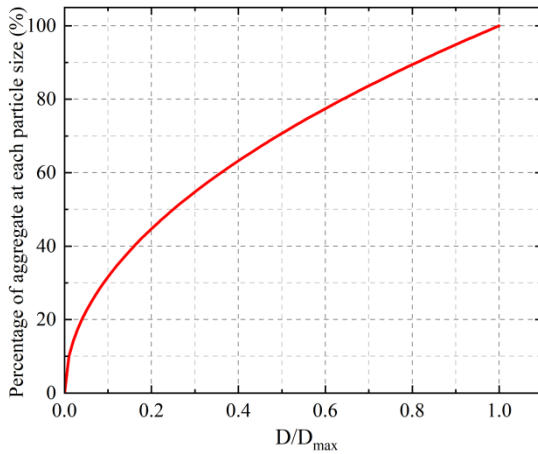


Fig. 1. Fuller grading curve

The Fuller grading equation is given by Equation (1)

$$P(d) = 100(d / d_{max})^n \tag{1}$$

In the formula:

P(d)—The cumulative percentage passing through a sieve with an aperture size of d

d<sub>max</sub>—The maximum size of aggregate particles

n—The exponent of the equation (n =0.45-0.70). The recommended range of n values is from 1/3 to 1/2. As the n value increases, the proportion of fine particles decreases, while the proportion of coarse particles increases. When n = 0.5, the corresponding curve represents the maximum density theoretical curve, with the minimum void ratio of the granular material, achieving a closely packed state. For a mixture of coarse aggregate, fine aggregate, and powder materials, mixing according to the Fuller curve proportion can achieve the closest packing with the minimum void ratio. After adding water and admixtures, flowable concrete can be obtained[7].

If the size distribution of aggregate particles is given by a common grading curve, then the volume fraction of each grading segment can be calculated as:

$$v_p [d_s, d_{s+1}] = \frac{P(d_s) - P(d_{s+1})}{P(d_{\max}) - P(d_{\min})} v_p \quad (2)$$

In the formula:

$v_p [d_s, d_{s+1}]$ —The volume fraction of aggregate within the size range[  $d_s, d_{s+1}$  ]

$d$ —The sieve aperture size

$d_{\max}, d_{\min}$ —The maximum and minimum sizes of coarse aggregate particles

### 3 Random Aggregate Model Generation

#### 3.1 Software Application Introduction

In the early days, the use of finite element analysis in concrete structure research was not widespread due to limitations in computational tools. With the development of computer technology, finite element analysis software has emerged continuously, and its accuracy has gradually improved, playing an important role in scientific research and engineering fields. Using these software tools can greatly increase efficiency, such as ANSYS, ABAQUS, OpenSees, etc. Abaqus software is a world-leading general-purpose finite element analysis software developed by SIMULIA, a subsidiary of Dassault Systèmes (DS). As a global leading finite element analysis tool, Abaqus software plays an important role in many engineering fields with its comprehensive functions, powerful solvers, a wide range of material models, and user-friendly interface. It can handle simple linear analyses to complex nonlinear problems and supports multi-physics coupling analysis, covering various aspects such as statics, dynamics, thermo-solid coupling, acoustics, and electromagnetic analysis. In particular, it has very strong Python secondary development capabilities, providing conditions for the establishment of random aggregate audit models.

#### 3.2 Random Aggregate Model Establishment

This study uses a spatial base sphere and employs point random shape control methods and planar topology techniques to achieve the spatial generation of polyhedral aggregates. The convexity of the random polyhedra is determined using vector methods, effectively avoiding the creation of aggregates with sharp angles and flaky shapes[3]. The specific steps and approach are as follows:

##### (1) Single aggregate construction

Generate  $n$  random vertices on a spatial sphere, with the generation of random vertices based on spherical coordinates, utilizing a random function to select random numbers. By controlling the minimum distance between vertices, ensure that the generated aggregate shape has a certain degree of irregularity and complexity, while avoiding vertices being too close or overlapping, which could affect the rationality of the model and computational efficiency. The implementation process is as follows.

$$\begin{aligned}
 z &= r_i \cos \beta_i \\
 x &= r_i \cos \alpha_i \sin \beta_i \\
 y &= r_i \sin \alpha_i \sin \beta_i
 \end{aligned}
 \tag{3}$$

Here,  $r_i$  represents the radius corresponding to the  $i$ -th matrix sphere, with its range corresponding to the size range of aggregate particle diameters as per the Fuller grading.  $\alpha$  is the azimuthal angle, which is the angle fluctuating within the XY plane, with a fluctuation range of  $[0, 2\pi]$ . Similarly,  $\beta$  is the polar angle, fluctuating within the YZ plane, with the same fluctuation range. After generating the vertices, the `itertools.combinations` function is used to perform combinations of any three vertices among all vertices to form a plane. To select valid planes (i.e., to avoid intersections and penetrations), we stipulate that:

① For each combination of three vertices, calculate the normal vector of the plane.

② Check if other vertices are on the same side of the plane. The specific method is to calculate the dot product of each vertex with the plane's normal vector. If the dot product is less than  $-1e-5$  (using  $-1e-5$  instead of 0 in the code is to handle floating-point precision issues in numerical calculations. In computers, there are certain precision limitations in the representation and calculation of floating-point numbers, which can lead to some values that should theoretically be zero having a small non-zero value in actual calculations), then the vertex is not on the same side of the plane, and it is an invalid plane.

③ If all vertices are on the same side of the plane, then add this plane combination to the list of valid face combinations.

The normal vector of a plane is calculated using the cross product of vectors, and normalization is required after the calculation to facilitate subsequent operations. Equation 4 represents the calculation of the plane's normal vector, Equation 5 represents the formula for calculating the magnitude (norm), and Equation 6 represents the normalization calculation.

$$\mathbf{n} = \begin{vmatrix} i & j & k \\ x_2 - x_1 & y_2 - y_1 & z_2 - z_1 \\ x_3 - x_1 & y_3 - y_1 & z_3 - z_1 \end{vmatrix}
 \tag{4}$$

Here,  $i$ ,  $j$ , and  $k$  are the unit vectors in the  $x$ ,  $y$ , and  $z$  directions, respectively, and each vertex is formatted as  $[x, y, z]$ .

Calculate the dot product of the normal vector with the first vertex; if the dot product is greater than  $\pi/2$ , then invert the normal vector to ensure consistent direction.

Given a normal vector  $\mathbf{n}=[a, b, c]$ , the formula for calculating its magnitude is:

$$\|\mathbf{n}\| = \sqrt{a^2 + b^2 + c^2}
 \tag{5}$$

The normalized normal vector is:

$$n_{\text{normalized}} = \frac{n}{\|n\|} = \left[ \frac{a}{\|n\|}, \frac{b}{\|n\|}, \frac{c}{\|n\|} \right] \tag{6}$$

As shown in Figure 2 is an illustration of the geometric identification during the aggregate construction process.

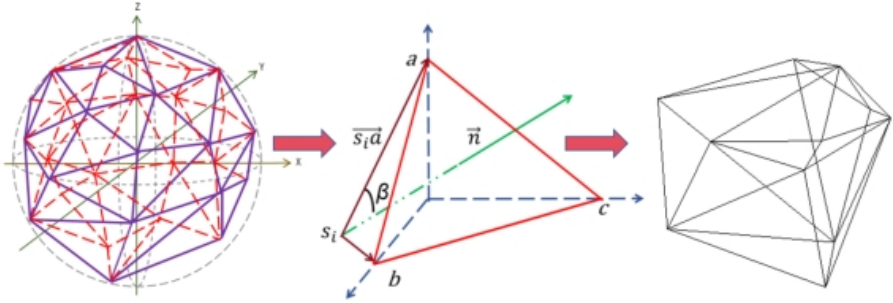


**Fig. 2.** Construction of the normal vector identification for a single aggregate

$$S_i a = (x_i, y_i, z_i) \tag{7}$$

$$\vec{n} = (x_n, y_n, z_n) \tag{8}$$

$$\beta = \arccos \left[ \frac{\overline{S_i a} \cdot \vec{n}}{|\overline{S_i a}| \cdot |\vec{n}|} \right] \tag{9}$$

After labeling and identifying the planes constructed from random vertices, use ABAQUS built-in WirePolyLine and CoverEdges commands to generate the edges and faces of the polyhedral aggregate. Finally, use the AddCells method to combine the generated faces into a closed polyhedral aggregate(As shown in Figure 3).

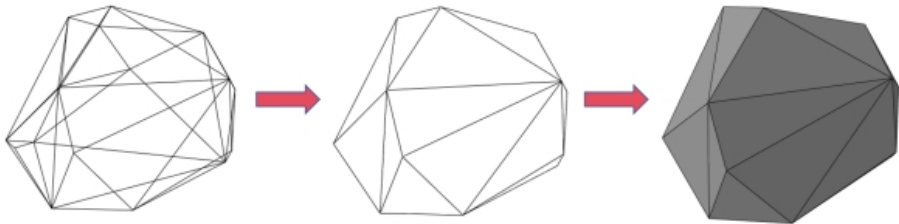


**Fig. 3.** The process of constructing a single aggregate is as follows

(2) Aggregate interference identification and batch placement

After completing the establishment of a single random aggregate model, the next step is to batch place all sizes of aggregates in the concrete area according to the Fuller grading, and generate the Interface Transition Zone (ITZ) and the mortar matrix. It should be noted that the batch placement process must meet the following requirements:

① Aggregates must not interfere or penetrate each other; otherwise, the placement is invalid.

② The boundary area between the aggregates and the concrete must not intersect; otherwise, it is considered that the aggregates are placed outside the concrete.

③ There must be an avoidance judgment between the aggregate placement area and the rebar placement area; aggregates must not intersect with the rebar.

The core identification process is as follows: The interference judgment between aggregates is achieved by calculating the distance between the centers of two aggregates and comparing it with the sum of their radii. If the distance is less than the sum of the radii, then the two aggregates interfere with each other.

$$d1 = \sqrt{(x_2 - x_1)^2 + (y_2 - y_1)^2 + (z_2 - z_1)^2} \quad (10)$$

$d_1$ : The Euclidean distance between the centers of the two aggregates.  $r_1$  and  $r_2$ : The radii of the two aggregates.

If the distance between the centers of two aggregates is less than the sum of their radii, it indicates that the two aggregates overlap or are in contact with each other, i.e., interference occurs (As shown in Figure 4).

Determining whether an aggregate interferes with a rectangular boundary is done by checking if the distance from the aggregate's center to the rectangular boundary is less than the aggregate's radius. If the distance is less than the radius, then the aggregate interferes with the rectangular boundary. After the boundary condition judgment, aggregates are placed in batches following the grading curve. It is important to note that the placement process must start with larger aggregates and then place smaller ones in the remaining space, proceeding in stages until the volume fraction requirements calculated by Fuller are met. Subsequently, using ABAQUS software's solid scaling function, the aggregates are enlarged and Boolean cuts are performed to obtain the ITZ and mortar matrix. With this, the entire three-dimensional mesoscale model of concrete is established (Figure 5 and figure 6).

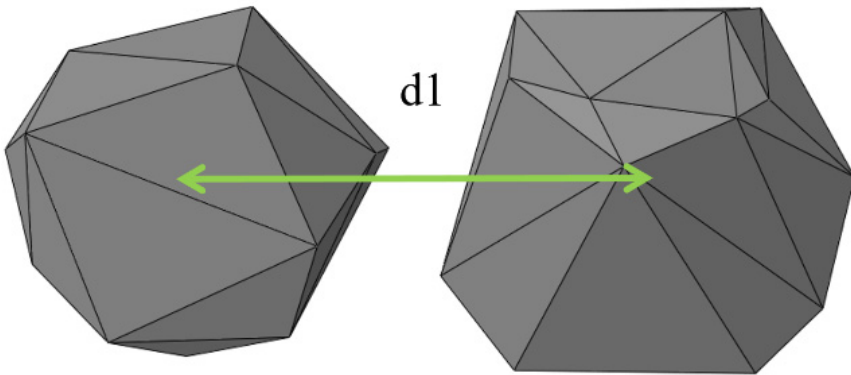


Fig. 4. Aggregate interference identification.

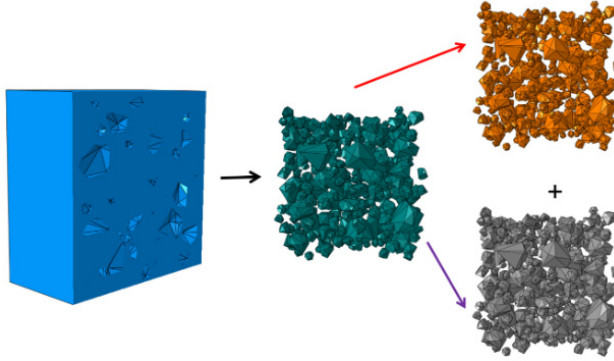


Fig. 5. three-phase mesoscale model

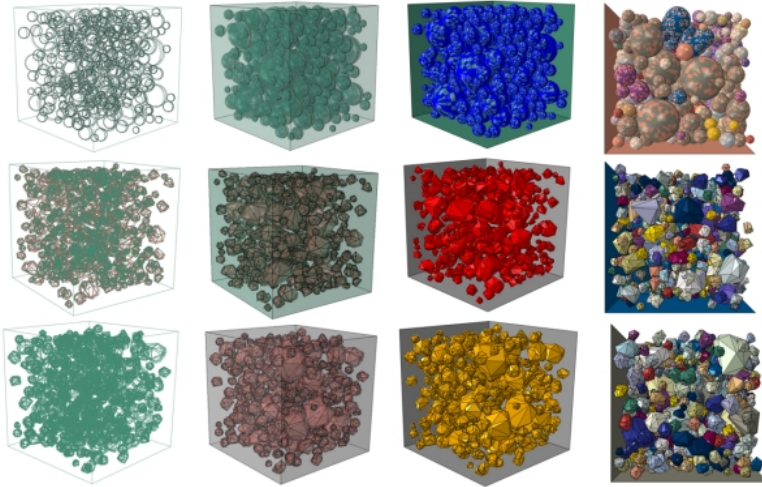


Fig. 6. Placement effect of spherical, 13-vertex, and 21-vertex polyhedral aggregates

## 4 Mesoscale Model Uniaxial Compression

### 4.1 CDP (Concrete Damaged Plasticity) Constitutive Model

The CDP model, in addressing the mechanical behavior of concrete materials, proposes that its failure mechanisms are primarily dominated by two modes: tensile cracking and compressive crushing. The model introduces two independent hardening variables—equivalent plastic tensile strain and equivalent plastic compressive strain—to dynamically describe the evolution of the yield surface or failure surface. The equivalent plastic tensile strain is associated with the accumulation of tensile failure, while the equivalent plastic compressive strain characterizes the nonlinear response of the material under compressive loads[6], Figure 7 presents the CDP constitutive expression.

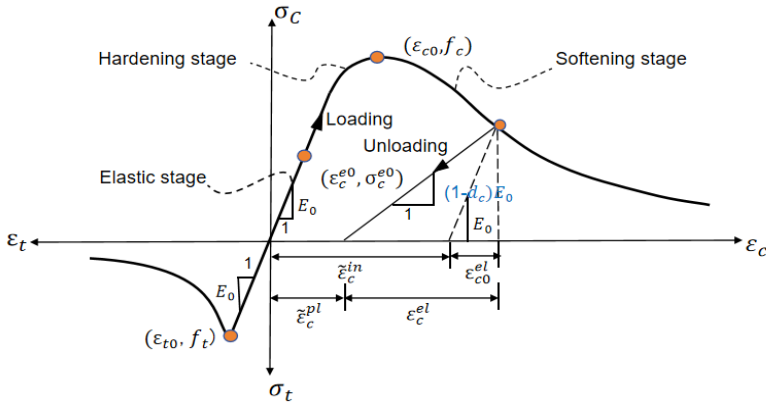


Fig. 7. The stress-strain relationship of concrete under uniaxial loading

Uniaxial Tensile Characteristics: Before reaching the tensile strength, the stress-strain relationship increases linearly, and the material undergoes no damage (damage factor  $d_t=0$ ), which is the elastic stage; after exceeding this point, the material enters a stage of stiffness degradation ( $d_t \in [0,1]$ ), where the stress gradually decreases with increasing strain, reflecting the degradation of load-bearing capacity due to crack propagation[4,5].

Uniaxial Compressive Characteristics: When the stress is below the proportional limit, the material behaves elastically (damage factor  $d_c=0$ ), which is the elastic stage; up to the peak stress, it is the elastoplastic deformation stage, where micro-cracks within the material gradually develop, representing a hardening process, i.e., the hardening stage; after exceeding this point, the compressive strength gradually decreases ( $d_c \in [0,1]$ ), reflecting the mechanical property degradation after the material is crushed, and the material begins to soften. The CDP model modifies the elastic response through the damage factor to establish the stress-strain relationship[4,5]:

$$\sigma_t = (1 - d_t)E_0(\epsilon_t - \epsilon_t^{pl}) \tag{11}$$

$$\sigma_c = (1 - d_c)E_0(\epsilon_c - \epsilon_c^{pl}) \tag{12}$$

Sure, here is the translation:

$d_t, d_c$  — Damage variables (0 for no damage, 1 for complete failure)

$E_0$  — Initial elastic modulus

$\epsilon_t, \epsilon_c$  — Total tensile strain, total compressive strain

$\epsilon_t^{pl}, \epsilon_c^{pl}$  — Equivalent plastic tensile strain, equivalent plastic compressive strain, combined with damage variables through evolution equations 13 and 14

In ABAQUS, users can define the softening stage of the stress-strain curve through the tensile cracking strain  $\epsilon_{tck}$  and the compressive inelastic strain  $\epsilon_{cin}$ . The ABAQUS embedded program can transform the tensile cracking strain  $\epsilon_{tck}$  and the compressive inelastic strain  $\epsilon_{cin}$  into equivalent plastic tensile and compressive strains according to equations (13) and (14)

$$\tilde{\varepsilon}_t^{pl} = \tilde{\varepsilon}_t^{ck} - \frac{d_t}{1-d_t} \frac{\sigma_t}{E_0} \quad (13)$$

$$\tilde{\varepsilon}_c^{pl} = \tilde{\varepsilon}_c^{in} - \frac{d_c}{1-d_c} \frac{\sigma_c}{E_0} \quad (14)$$

$$\tilde{\varepsilon}_t^{ck} = \varepsilon_t - \sigma_t / E_0 \quad (15)$$

$$\tilde{\varepsilon}_c^{in} = \varepsilon_c - \sigma_c / E_0 \quad (16)$$

#### 4.2 Failure Strength and Damage Morphology of Mesoscale Models of Concrete with Aggregates of Different Shapes

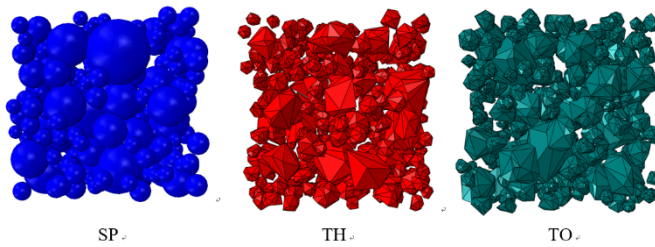


Fig. 8. Different Aggregate Shape Models

To verify the differences in strength and failure patterns caused by aggregate shape in the mesoscale model of Rubberized Self-Compacting Concrete (BRSC), we have established 100mm cubic concrete blocks with spherical aggregates (SP), 13-face polyhedral aggregates (TH), and 21-face polyhedral aggregates (TO). The 100mm size will reduce the number of mesh divisions and shorten computational costs. According to the "Standard for Testing and Evaluation of Concrete Strength" GB/T 50107-2010, multiplying the strength of the 100mm cube by 0.95 can yield the strength of the standard 150mm cube. The thickness of the Interface Transition Zone (ITZ) is 0.3-1.5mm. Figure 8 illustrates aggregates of different shapes.

**Mortar Matrix:** Based on the values from reference [9,10], it is assumed that the ratio of compressive strength to tensile strength is approximately 10:1.

**ITZ Parameters:** Initially, the strength of the ITZ (Interface Transition Zone) is set to be 50% to 80% of the mortar strength, and the elastic modulus is set to be 30% to 60% of the mortar's. The thickness of the ITZ is 0.05-0.1 mm.

After the model is established, meshing is required. In fact, the finite element method is a theory based on the variational principle and the weighted residual method, which discretizes continuous partial differential equations into a system of algebraic equations. Meshing is the foundation for achieving this discretization, where physical quantities within each element are approximated by interpolation functions, thereby forming the global stiffness matrix and load vector, transforming the continuous problem into a discrete problem for solution. In the ABAQUS software, three-dimensional mesh elements include hexahedral elements (Hex), tetrahedral elements (Tet), wedge elements

(Wedge), and hexahedral-dominated elements (Hex-dominated), etc. Hex represents a regular hexahedral structure with high computational accuracy, suitable for regular geometric shapes. Wedge is a triangular prism shape, suitable for transition areas or special geometric shapes.

Hex-dominated is mainly composed of hexahedral elements, with wedge elements allowed in transition areas, balancing accuracy and flexibility, and is needed for areas transitioning from regular to complex meshes. Tet, on the other hand, has high flexibility and is suitable for complex geometric shapes in three-dimensional structures. In this study, for a large number of complex structures, we use tetrahedral meshes, and for regular structures, we use hexahedral meshing.

In this uniaxial loading test, we first conducted a mesh sensitivity analysis on a 100mm concrete model with a 13-face polyhedral (TH) aggregate. Rigid steel plates were used as end caps, with the bottom plate fully fixed after applying a coupling point, and the top plate was subjected to displacement loading through point-to-surface coupling, with a loading displacement of 0.7mm(As shown in Figure 9). The interaction between the steel plate and the concrete was set to normal hard contact and tangential penalty function friction; The figure shows the boundary conditions and loading.

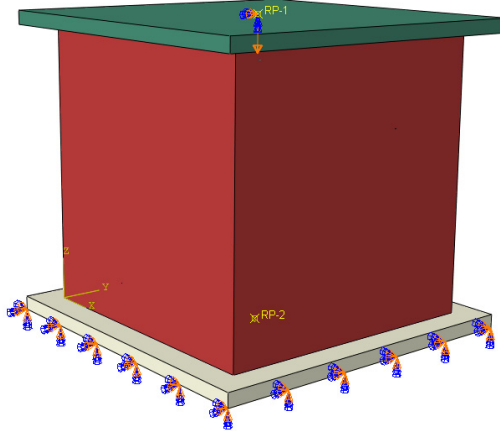


**Fig. 9.** Uniaxial Loading Displacement Settings and Boundary Conditions

From the above theory, it is known that the essence of the finite element method is a kind of discretization technique. In theory, as the mesh becomes finer, the results of finite element analysis will gradually approach the true solution. However, after the number of elements reaches a certain level, the improvement in the accuracy of the computational results becomes insignificant and may even stabilize. Through mesh sensitivity analysis, an appropriate mesh density can be found, ensuring that the computational results converge within an acceptable error range while avoiding the waste of computational resources due to excessive mesh refinement[8-10]. In the international academic community, obtaining a mesh-independent solution is a basic requirement for

accepting numerical computation papers. By progressively refining the mesh and comparing the computational results under different mesh densities, one can determine whether the results are independent of the mesh division. Therefore, before obtaining objective numerical results, we should conduct a mesh sensitivity analysis. In this study, we use a concrete model with a 13-face polyhedral aggregate as an example for analysis to determine an appropriate mesh density, which can then be generalized to other model analyses. The figure shows different mesh sizes of 3mm, 2mm, and 1mm(As shown in Figure 10). We gradually refine the mesh from coarser to finer and repeatedly simulate and compare the results.

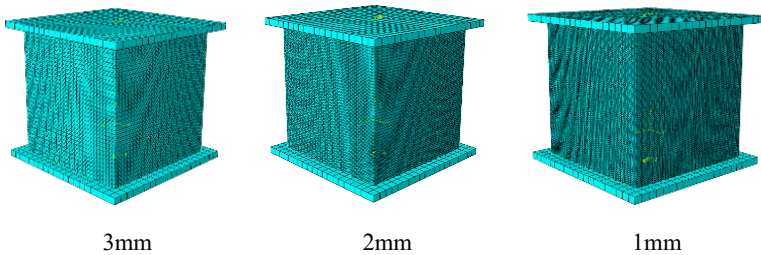
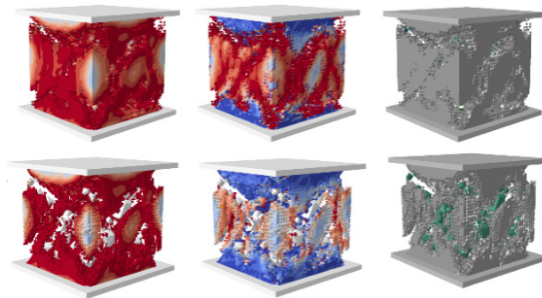
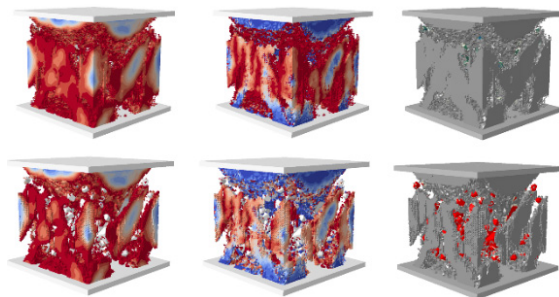


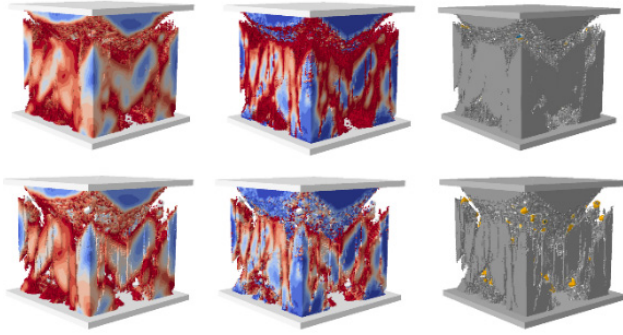
**Fig. 10.** TH with Different Mesh Elements



(a) Damage Pattern Distribution Corresponding to 3mm Mesh



(b) Damage Pattern Distribution Corresponding to 2mm Mesh



(c) Damage Pattern Distribution Corresponding to 1mm Mesh

**Fig. 11.** Damage Evolution Diagram of Models with Different Mesh Elements

By setting the removal of elements with stiffness degradation reaching 0.88 and 0.9, we can obtain the distribution of damage morphology after compression, tension, and the crushing failure of concrete. That is, as shown in Figure 11, from left to right, they represent compression damage, tension damage, and crushing failure, respectively. The top and bottom rows correspond to the damage distribution after the element damage reaches 0.88 and 0.9, respectively.

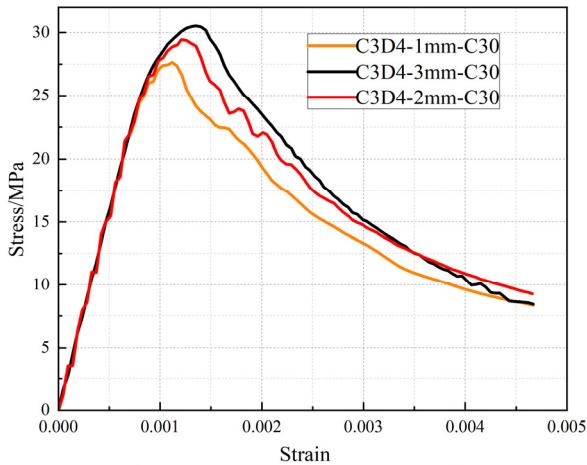
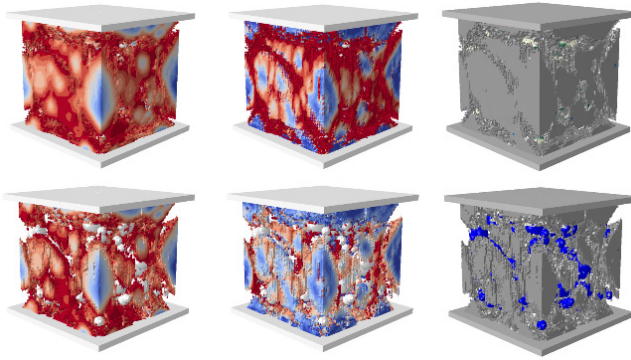
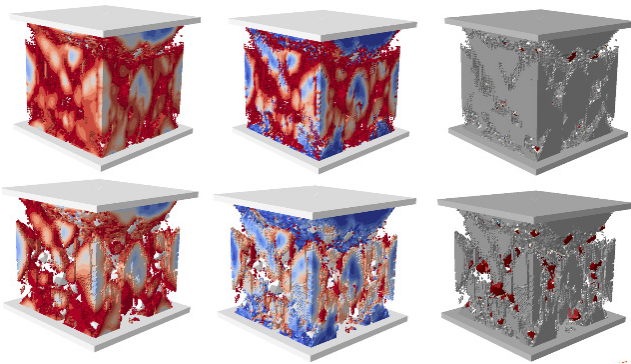


**Fig. 12.** Stress-Strain Curves for Different Mesh Sizes

All curves show a typical concrete stress-strain relationship(As shown in Figure 12): stress increases linearly with strain initially, then declines after peaking. The 1mm mesh curve declines slowly post-peak, indicating residual stress capacity after failure. The 2mm and 3mm curves decline faster, suggesting quicker loss of load-bearing capacity and some distortion of actual failure. Balancing accuracy and efficiency, we selected a 2mm mesh for further analysis.



(a) SP Damage Pattern



(b) TO Damage Pattern

**Fig. 13.** Damage and Failure of Models with Different Aggregate Shapes

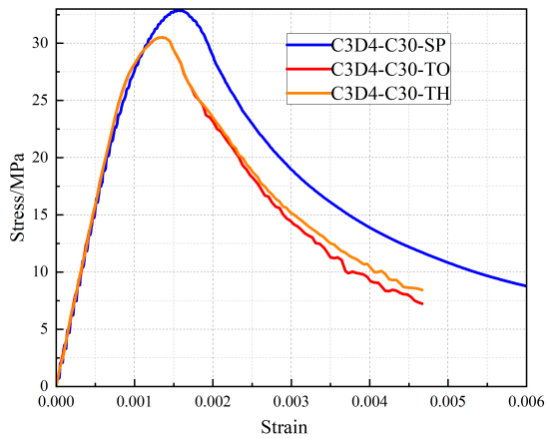


**Fig. 14.** Strength Analysis Chart for Different Shapes

The Figure 14 show that all types of aggregate concrete exhibit a typical stress-strain relationship with similar mechanical behavior, including an elastic phase, plastic phase, and failure phase, characterized by internal crack formation and propagation along the loading direction under compression (As shown in Figure 13).

## 5 Conclusions

This study has successfully established a three-dimensional mesoscale model of concrete and simulated its uniaxial mechanical behavior to analyze the damage and failure processes. The research has demonstrated that the finite element method, particularly at the mesoscale, is an effective tool for capturing the complex behavior of concrete under load, including crack propagation, stiffness degradation, and stress distribution.

(1) **Stress-Strain Relationship:** All aggregate concrete models demonstrated a typical stress-strain relationship, with stress increasing linearly initially and then decreasing gradually after reaching the peak value. This behavior was consistent across different aggregate shapes, indicating fundamental similarities in their mechanical behavior.

(2) **Damage and Failure Modes:** The study showed distinct stress-strain relationships and failure modes for concrete with different aggregate shapes. Concrete with spherical aggregates had the highest peak strength and retained some load-bearing capacity after failure, whereas concrete with irregular polyhedral aggregates exhibited faster crack propagation and lower residual strength.

(3) **Mesh Sensitivity Analysis:** Through mesh sensitivity analysis, an appropriate mesh density was determined to ensure that the computational results converged within an acceptable error range without excessive refinement. Balancing accuracy and computational efficiency is crucial for practical applications.

(4) **Aggregate Shape Impact:** The shape of aggregates significantly affected the mechanical properties of concrete. Spherical aggregates outperformed irregular polyhedral aggregates in terms of strength and residual capacity.

(5) **Practical Implications:** The findings provide a theoretical basis for the engineering design and performance evaluation of concrete structures. Understanding the impact of aggregate shape on concrete behavior can guide material selection and design strategies to enhance the structural integrity and durability of concrete constructions.

**Limitations and Future Outlook:**

(1) The study assumes simplified representations of aggregate shapes and the interface transition zone (ITZ), potentially neglecting complex factors such as interfacial bonding characteristics between aggregates and cement paste. This may lead to discrepancies between simulation results and real-world concrete behavior.

(2) The study primarily relies on numerical simulations without sufficient experimental validation, which may reduce the credibility of the results.

(3) The findings provide theoretical support for concrete structure design and performance evaluation, particularly in optimizing aggregate selection to enhance the strength and durability of concrete structures.

(4) The mesoscale modeling approach can be extended to multiscale analysis, integrating microscale and macroscale models to offer a more comprehensive tool for predicting and optimizing concrete performance.

## References

1. Jin L, Liu M, Zhang R, Du X. 3D meso-scale modelling of the interface behavior between ribbed steel bar and concrete. *Engineering Fracture Mechanics*, 2020, 239: 107291.
2. Jin L, Yu W, Du X, Zhang S, Li D. Meso-scale modelling of the size effect on dynamic compressive failure of concrete under different strain rates. *International Journal of Impact Engineering*, 2019, 125: 1-12.
3. Zhou G, Xu Z. 3D mesoscale investigation on the compressive fracture of concrete with different aggregate shapes and interface transition zones. *Construction and Building Materials*, 2023, 393: 132111.
4. Lee J, Fenves GL. Plastic-damage model for cyclic loading of concrete structures. *Journal of Engineering Mechanics*, 1998, 124: 892-900.
5. Lubliner J, Oliver J, Oller S, et al. A plastic-damage model for concrete. *International Journal of Solids & Structures*, 1989, 25(3): 299-326.
6. Chen F, Gao C, Jin L, Du X. Dynamic responses of radiation-induced heavyweight concrete subjected to biaxial compression. *International Journal of Mechanical Sciences*, 2023, 257: 108519.
7. Wriggers P, Mofteh S. Mesoscale models for concrete: Homogenisation and damage behaviour. *Finite Elements in Analysis and Design*, 2006, 42(7): 623-636.
8. Naderi S, Tu W, Zhang M. Meso-scale modelling of compressive fracture in concrete with irregularly shaped aggregates. *Cement and Concrete Research*, 2021, 140: 106317.
9. Zhang R, Jin L, Du X. Three-dimensional meso-scale modelling of failure of steel fiber reinforced concrete at room and elevated temperatures. *Construction and Building Materials*, 2021, 278: 122368.
10. Ouyang H, Chen X. 3D meso-scale modeling of concrete with a local background grid method. *Construction and Building Materials*, 2020, 257: 119382.

**Open Access** This chapter is licensed under the terms of the Creative Commons Attribution-NonCommercial 4.0 International License (<http://creativecommons.org/licenses/by-nc/4.0/>), which permits any noncommercial use, sharing, adaptation, distribution and reproduction in any medium or format, as long as you give appropriate credit to the original author(s) and the source, provide a link to the Creative Commons license and indicate if changes were made.

The images or other third party material in this chapter are included in the chapter's Creative Commons license, unless indicated otherwise in a credit line to the material. If material is not included in the chapter's Creative Commons license and your intended use is not permitted by statutory regulation or exceeds the permitted use, you will need to obtain permission directly from the copyright holder.

